Nucleic Acids Research, 1994, Vol. 22, No. 23 **4979–4982**

Sequence-specific DNA double-strand breaks induced by triplex forming ^{125}I labeled oligonucleotides

Igor G.Panyutin* and Ronald D.Neumann
Department of Nuclear Medicine, Clinical Center, National Institutes of Health, Bethesda, MD 20892, USA

Received August 12, 1994; Revised and Accepted October 17, 1994

ABSTRACT

A triplex-forming oligonucleotide (TFO) complementary to the polypurine–polypyrimidine region of the *nef* gene of the Human Immunodeficiency Virus (HIV) was labeled with ^{125}I at the C5 position of a single deoxycytosine residue. Labeled TFO was incubated with a plasmid containing a fragment of the *nef* gene. Decay of ^{125}I was found to cause double-strand breaks (DSB) within the *nef* gene upon triplex formation in a sequence specific manner. No DSB were detected after incubation at ionic conditions preventing triplex formation or when TFO was labeled with ^{32}P instead of ^{125}I. Mapping DSB sites with single base resolution showed that they are distributed within 10 bp of a maximum located exactly opposite the position of the [^{125}I] IdC in the TFO. We estimate that on average the amount of DSB produced per decay is close to one.

INTRODUCTION

Decay of Auger electron emitters, such as ^{125}I, incorporated in one of the DNA strands, is known to cause double-strand breaks (DSB) (1,2). In contrast to X-rays and high linear energy transfer (LET) emitters, Auger emitters deposit high doses of radiation within a range of 1 to 10 nm from the site of decay [see (3) and references therein]. Thus, decay of ^{125}I produces DSB distributed within 10 bp around the base containing the radioisotope without damaging the rest of the molecule (2,4,5). Although electrons emitted in an Auger cascade display very low energy (20–250 eV) (3), when incorporated into cellular DNA, ^{125}I and other Auger-emitters are extremely radiotoxic and produce survival curves typical of high LET radiation (6–10). However, iodine-125-labeled DNA-binding drugs were found to be considerably less radiotoxic as compared to [^{125}I]-deoxyuridine given as a precursor of DNA synthesis (11). Therefore, one might expect that decay of ^{125}I produces less damage in DNA if the radionuclide is placed *in trans* to the double helix.

Polypurine and polypyrimidine oligonucleotides can bind to the major groove of complementary duplexes without significant distortion of the latter by forming triple helical structures or triplexes (12,13). Thus, triplex-forming oligonucleotides (TFO) provide us with a convenient tool to study the sequence-specific action of ^{125}I decay.

Herewithin we present our studies on the efficiency and distribution of DSB induced by decay of ^{125}I incorporated into TFO. As a model, we used binding of a polypyrimidine TFO to a polypurine–polypyrimidine sequence from the *nef* gene of HIV (14,15). We show that even after being incorporated into TFO and, therefore, located *in trans* to the double helix, ^{125}I is able to produce DSB with an efficiency of 0.8 DSB per decay; and that DSB are distributed within a very short distance around the radioisotope decay site.

MATERIALS AND METHODS

DNA

Plasmid pCR12713Nef containing a 750 bp PCR fragment of HIV DNA from the region of the *nef* gene in *Eco*RI site of pCRII vector (Invitrogen) was kindly provided by Dr A.Malykh (NCI). Plasmid DNA was purified from *E.coli* cells using a Maxiprep purification kit (Qiagene). Digestion with restriction enzymes *Eco*RI and *Bgl*II (New England Biolabs) were performed according to the manufacturer's instructions.

[^{125}I] IdC containing TFO

Oligonucleotides were synthesized on a ABI-394 DNA synthesizer (Applied Biosystems). [^{125}I] IdCTP (2200 Ci/mmol) and α[^{32}P]dCTP (6000 Ci/mmol) (DuPont-NEN) were incorporated into TFO by T7 DNA polymerase (Sequenase 2, USB) using a complementary strand as a template and a 19 nt long primer. The sequences of the template and the primer are: 5′-GGGAAGGGAAGGGGGGAAAAGAAAATCGCTTCATC and 5′-TTTTCTTTTCCCCCCTTCC. After annealing of the primer, the reaction was initiated by addition of T7 DNA polymerase and ^{125}I or ^{32}P labeled dCTP. Then, a 500-fold excess of cold dNTP's was added to fill in the end of the duplex. The sequence of the TFO is 5′-TTTTCTTTTCCCCCCTTCC-([^{125}I]IdC or [^{32}P]dC)-TTCCC. Template and TFO were separated by gel electrophoresis in denaturing polyacrylamide gel (PAG). The TFO band was cut and TFO was eluted as previously described (16). The radioactivity of the samples was

*To whom correspondence should be addressed

measured on Packard 5650 Auto-Gamma or A4530D scintillation counter. We estimated that less than 10% of the TFO in the final preparation contained [^{125}I]IdC. The [^{32}P]TFO sample was diluted with cold TFO to the same specific activity as [^{125}I]IdC.

Formation of DNA triplexes

Plasmid pCR12713Nef was digested with *Eco*RI and incubated with TFO in 10 μl of TA (50 mM Na Acetate, pH 5, 3 mM Mg Acetate) or TE (10 mM Tris−HCl, pH 8 and 1 mM EDTA) buffer at 37°C for 30 min. The final concentration of plasmid DNA was 100 μg/ml. The formation of the triplexes was confirmed by gel electrophoresis in 2% agarose gel at 4°C using TA as an electrode buffer. Samples were kept frozen at −20°C.

Analysis of DSB

The frozen samples were thawed on ice and 1 μl of each was diluted in 20 μl of TES buffer (50 mM Tris−HCl, pH 7.5, 50 mM NaCl, 1 mM EDTA). Plasmid DNA was separated from the TFO by gel filtration through Microspin S-300 columns (Pharmacia) and in some cases cut with *Bgl*II. Plasmid DNA was labeled at the 3′ end with α[^{33}P]dATP and Klenow fragment of DNA polymerase I (USB) or at the 5′ end with γ[^{32}P]ATP and T4 Polynucleotide Kinase (USB) and analyzed in native or denaturing (PAG). Gels were autoradiographed on Kodak XAR 2 film or quantitated using a Phosphorimager (Molecular Dynamics). Maxam−Gilbert sequencing reactions were performed as described (17).

RESULTS

Binding of TFO to a target sequence

Plasmid pCR12713Nef was cut with *Eco*RI restriction enzyme giving rise to two fragments: a 3.9 kbp fragment containing vector sequence and a 0.75 kbp fragment containing the *nef* sequence (Fig. 1). Six nCi and 60 nCi of [^{125}I]TFO were mixed with 1 μg of *Eco*RI digested plasmid in 10 μl of TA buffer (pH 5) to form triplexes. Formation of the polypyrimidine−polypurine−polypyrimidine triplexes requires protonation of cytosine residues (18). Triplexes of this type are stable at low pH and become unstable as the pH rises (19). As a negative control, we mixed 60 nCi of [^{125}I]TFO with 1 μg of *Eco*RI cut plasmid in TE buffer (pH 8). We also prepared the same samples containing [^{32}P]TFO under binding and nonbinding conditions. All samples were incubated for 10 min at 37°C. One μl of each sample was analyzed by electrophoresis in a 2% agarose gel using TA as an electrode buffer. An autoradiograph of the gel is shown on Figure 2. All [^{125}I]TFO were bound to the *nef*-containing insert when 6 nCi of [^{125}I]TFO was used and more than 90% was bound when 60 nCi of [^{125}I]TFO was used (lanes 1, 2). As expected, no binding was observed at pH 8 (TE buffer, lane 3). The same results were obtained for [^{32}P]TFO (lanes 4, 5). TFO did not bind to the 3.9 kbp vector fragment under any conditions (Fig. 2), which confirms the specificity of binding.

Mapping of DSB

Samples with [^{125}I]TFO and [^{32}P]TFO were kept at −20°C for 14 and 56 days to accumulate decays. Aliquots of the samples were ^{33}P-labeled at the 3′ end (14 days), and at the 3′ or 5′ ends (56 days) of the *Eco*RI sites, and analyzed by electrophoresis in 6% native and denaturing PAG. Results of such an analysis after 56 days are shown in Figure 3A and B. When [^{125}I]TFO was bound to the *nef*-containing insert, two fragments of approximately 420 bp and 330 bp long appeared (lanes 1 and 6). These fragments resulted from the DSB produced by decay of [^{125}I]IdC and mapped to the expected position in the polypurine−polypyrimidine region of the *nef* gene. No DSB were observed after incubation with [^{125}I]TFO in nonbinding conditions (lane 2) or with [^{32}P]TFO in both binding and nonbinding conditions (lanes 3 and 4).

Efficiency of DSB

The percentage of molecules that have received DSB was measured as the ratio of the radioactivity of the 420 bp and 330 bp fragments to the sum of the radioactivity of the 420 bp, 330 bp and 750 bp fragments. In denaturing PAG this ratio for the 420 nt 3′-*Eco*RI-labeled fragment corresponds to the percentage of the breaks in the pyrimidine strand. For the 330 nt fragment,

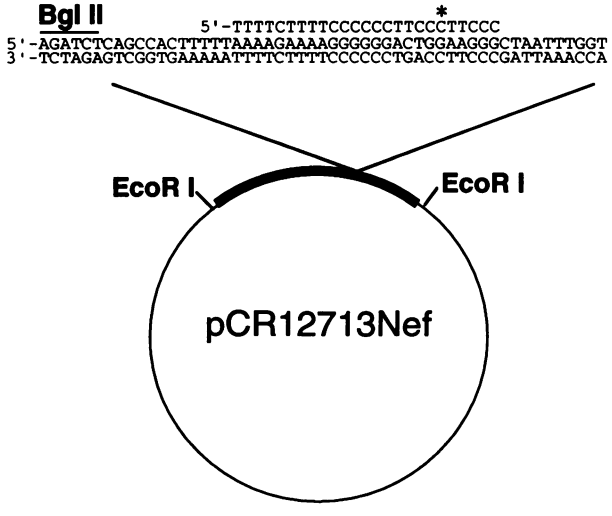

Figure 1. Map of the pCR12713Nef plasmid. The 750 bp PCR generated insert between two *Eco*RI sites is shown in bold. The sequences of the polypurine−polypyrimidine tract in the insert and TFO are shown at the top.

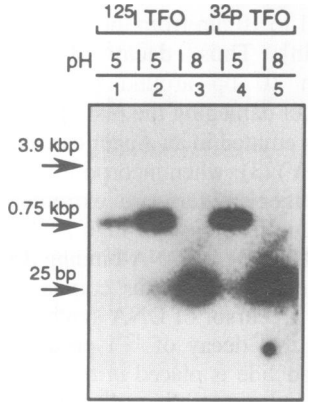

Figure 2. Binding of TFO to *Eco*RI-digested pCR12713Nef plasmid. Lane 1: 6 nCi of [^{125}I]TFO in TA buffer (binding conditions); lane 2: 60 nCi of [^{125}I]TFO in TA buffer; lane 3: 60 nCi of [^{125}I]TFO in TE buffer (nonbinding conditions); lane 4: 60 nCi of [^{32}P]TFO in TA buffer; lane 5: 60 nCi of [^{32}P]TFO in TE buffer. Length of the fragments in base pairs is shown on the left.

it corresponds to the percentage of the breaks in the purine strand of the duplex. In the case of the 5′-*Eco*RI-labeled fragments, the 420 nt fragment corresponds to the breaks in the purine and the 330 nt in the pyrimidine strand. Since intact 750 nt fragments labeled on either the purine or pyrimidine strand comigrate in denaturing PAG, the intensity of the corresponding band was divided by 2 to calculate the percentage of the single-stranded breaks.

Results of these measurements are summarized in Table 1. Errors were determined to be no more than ± 20%. The fact that the amount of DSB is very close (within experimental error) to the amount of single-strand breaks for both strands proves that the majority of the breaks are double-strand. The initial specific activity of [^{125}I]TFO was 1.3×10^4 dpm/ng. Thus the number of decays in the sample containing 10 ng of TFO accumulated for 56 days is 7.8×10^9. The number of target molecules in the

Table 1. Percentage of the DNA molecules cleaved by ^{125}I decay

	5′-end labeled Strand			3′-end labeled Strand		
	Pur.	Pyr.	DSB	Pur.	Pyr.	DSB
14 days	--	--	--	0.8%	1.0%	0.8%
56 days	4.0%	3.8%	3.6%	3.5%	3.6%	2.8%

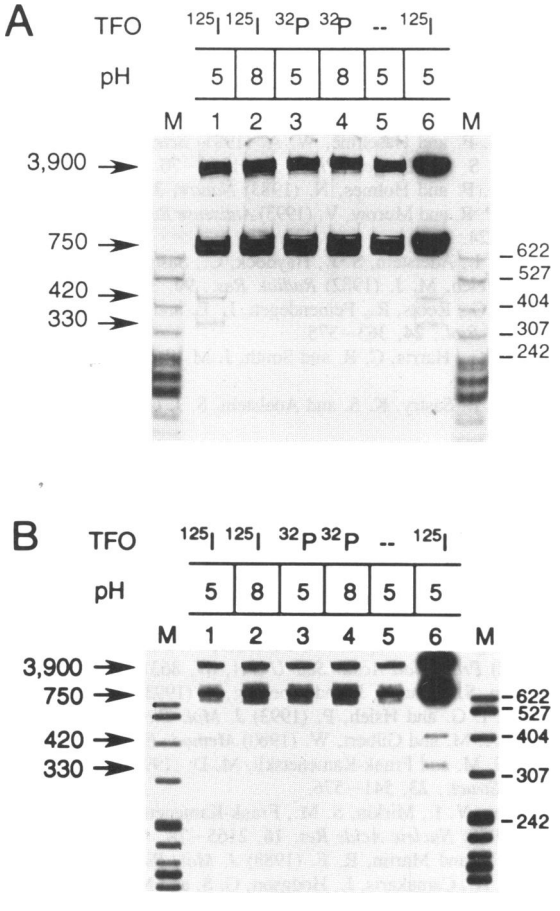

Figure 3. Native (**A**) and denaturing (**B**) PAG analysis of DSB in pCR12713Nef plasmid. Length of the fragments in base pairs (A) and nucleotides (B) is shown on the left. M: molecular weight markers (lengths are shown on the right). Lane 1: 60 nCi of [^{125}I]TFO in TA buffer; lane 2: 60 nCi of [^{125}I]TFO in TE buffer (nonbinding conditions); lane 3: 60 nCi of [^{32}P]TFO in TA buffer; lane 4: 60 nCi of [^{32}P]TFO in TE buffer; lane 5: no TFO added control; lane 6: 60 nCi of [^{125}I]TFO in TA buffer, sample was labeled at the 5′ ends for analysis. pH 5 at the top indicates binding and pH 8 nonbinding conditions.

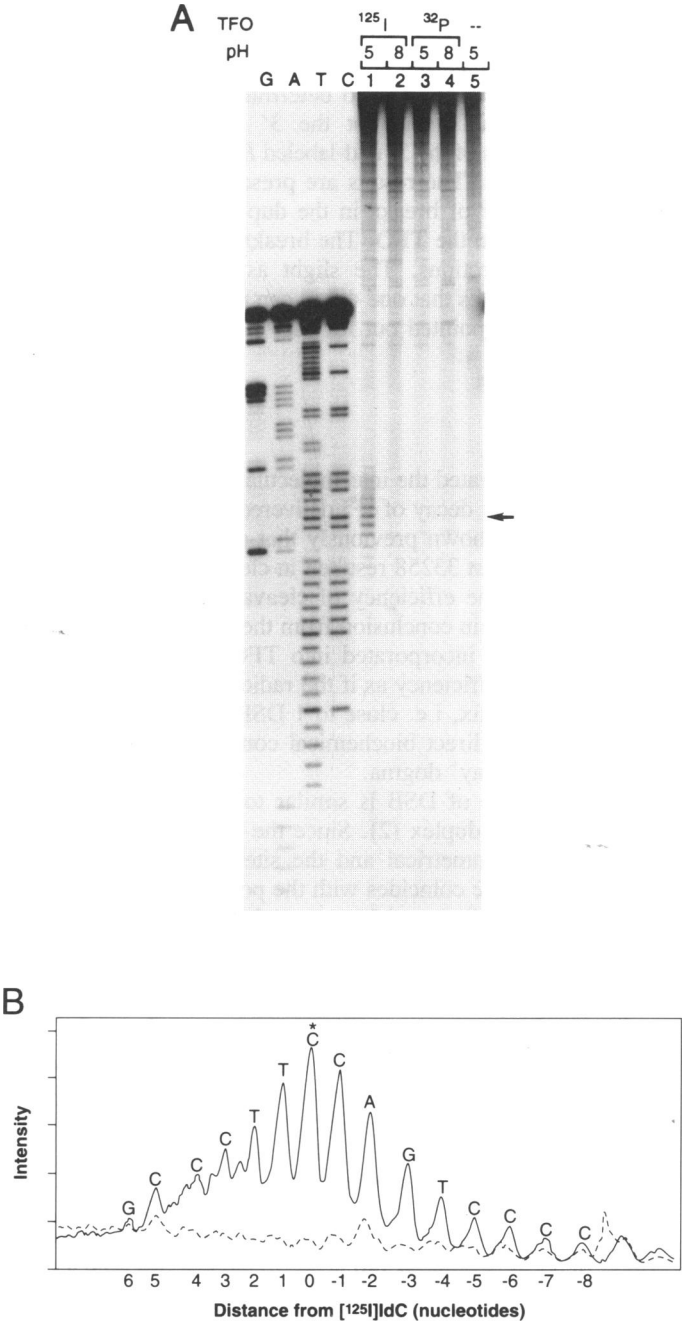

Figure 4. Distribution of DSB sites in pCR12713Nef plasmid. (**A**) G,A,T,C — G, A+G, C+T and C Maxam−Gilbert sequencing ladders of the 3′-*Bgl*II labeled *Bgl*II−*Eco*RV fragment. Lane 1: 60 nCi of [^{125}I]TFO in TA buffer; lane 2: 60 nCi of [^{125}I]TFO in TE buffer (nonbinding conditions); lane 3: 60 nCi of [^{32}P]TFO in TA buffer; lane 4: 60 nCi of [^{32}P]TFO in TE buffer; lane 5: no TFO added control. Arrow indicates the position of maximum cleavage. (**B**) Distribution of the intensities of the bands in lane 1 and lane 2. DNA bases corresponding to the bands are shown at the top. Distance from the maximum is shown at the bottom.

sample was 2×10^{11}. Multiplying this number by the percentage of breaks (Table 1), and assuming that all TFO's were bound to the targets (Fig. 2, line 2), we found that on average one decay produced 0.8 DSB.

Analysis of DSB on the sequencing level

We analyzed the distribution of DSB in polypurine–polypyrimidine region with single-base resolution. Plasmid DNA was cut with *Bgl*II restriction enzyme which has its only recognition site within the insert. This site is 15 bp away from the 5′ end of the targeted sequence (Fig. 1). To determine the positions of the breaks, DNA was labeled at the 3′ end. Maxam–Gilbert sequencing ladders of the 3′ end-labeled *Bgl*II–*Eco*RV fragment served as markers. The results are presented in Figure 4. The maximum number of breaks in the duplex corresponds to the [^{125}I]dC position in the TFO. The breaks are distributed within 5 nt in both directions. The slight asymmetry of the DSB distribution indicates that one decay can produce more than one DSB as has been pointed out for the ^{125}I labeled duplex DNA molecules (2).

DISCUSSION

We have demonstrated the intermolecular site-specific cleavage of duplex DNA by decay of ^{125}I delivered to the target sequence by TFO. It was shown previously that after binding to DNA, ^{125}I-labeled Hoechst 33258 resulted in cleavage of DNA strands (20). However, the efficiency of cleavage per decay was not measured. The main conclusion from the data presented here is that decay of ^{125}I incorporated into TFO produces DSB with almost the same efficiency as if the radionuclide were a part of a DNA double helix, i.e. close to 1 DSB per decay (1). These data are the first direct biochemical confirmation of the 'one-break-per-one-decay' dogma.

The distribution of DSB is similar to that observed for the ^{125}I-labeled DNA duplex (2). Since the distribution of DSB is only slightly asymmetrical and the site corresponding to the maximum cleavage coincides with the position of [^{125}I]IdC, we believe that the majority of decays produce only one DSB. The observed distribution of DSB, in this case, reflects directionality of decay action. Although the mechanism of strand breakage by decay of Auger emitters is still unclear, the comparison of the distribution of DSB with microdosimetry calculations may shed some light on this complicated problem. It is also worth noting that the bands corresponding to decay-induced breaks comigrate with the products of Maxam–Gilbert sequencing reactions and, therefore, may have the same chemical structure, i.e. corresponding base and deoxyribose are completely eliminated and the 5′ end has terminal phosphate group (17).

The low total yield of DSB (4% of duplexes were cut after 56 days of decay accumulation) is due to the fact that only a small fraction of the TFO contained radionuclide after our labeling procedure. Considerably higher specific activity [^{125}I]TFO could be achieved if multiple incorporation of ^{125}I-labeled precursor were allowed. In this study we addressed questions of efficiency and distribution of the breaks. Both of these parameters would be difficult to measure in the case of multiple incorporation of ^{125}I. The specific activity of [^{125}I]TFO was also reduced during denaturation and following strand separation in denaturing PAG. We are working now on a chemical method of direct incorporation of ^{125}I into TFO which we believe will allow us to obtain a higher specific activity.

Labeled to a high specific activity with Auger emitters, TFO may be useful in different applications requiring sequence-specific cleavage of a DNA molecule from large scale genome mapping to gene therapy. For instance, the TFO studied here may be used for targeting DSB to the HIV proviral sequence residing in the genome. DSB produced by the decay of ^{125}I have been shown to be difficult to repair, and usually cause deletions up to several kbp in size (21). Due to the very short range of the damage, the rest of the genome DNA as well as DNA of the host cell that does not contain proviral DNA will receive a significantly smaller dose of radiation produced by the higher energy portion of ^{125}I decay spectrum (22,23). The long half-life (60 days) of ^{125}I is an obvious disadvantage of using this radionuclide, especially in experiments with living cells. We believe that other Auger emitters such as ^{131}I or ^{77}Br, with shorter half-lives can substitute for ^{125}I in *in vivo* experiments.

ACKNOWLEDGEMENTS

We thank Dr Andrei Malykh for pCR12713Nef plasmid, Dr Mary McManaway for oligonucleotide syntheses and Dr Peggy Hsieh for critical comments on the manuscript.

REFERENCES

1. Krisch, R. E. and Sauri, C. J. (1975) *Int. J. Radiat. Biol. Relat. Stud. Phys. Chem. Med.*, **27**, 553–60.
2. Martin, R. F. and Haseltine, W. A. (1981) *Science*, **213**, 896–8.
3. Sastry, K. S. (1992) *Med. Phys.*, **19**, 1361–70.
4. Martin, R. F. and Holmes, N. (1983) *Nature*, **302**, 452–4.
5. England, P. R. and Murray, V. (1993) *Antisense Research and Development*, **3**, 219–224.
6. Kassis, A. I., Adelstein, S. J., Haydock, C., Sastry, K. S., McElvany, K. D. and Welch, M. J. (1982) *Radiat. Res.*, **90**, 362–73.
7. Burki, H. G., Roots, R., Feinendegen, L. E. and Bond, V. P. (1973) *Int. J. Radiat. Biol.*, **24**, 363–375.
8. Hofer, K. G., Harris, C. R. and Smith, J. M. (1975) *Int. J. Radiat. Biol.*, **28**, 225–241.
9. Kassis, A. I., Sastry, K. S. and Adelstein, S. J. (1987) *Radiat. Res.*, **109**, 78–89.
10. Makrigiorgos, G. M., Berman, R. M., Baranowska-Kortylewicz, J., Bump, E., Humm, J. L., Adelstein, S. J. and Kassis, A. I. (1992) *Radiat. Res.*, **129**, 309–14.
11. Kassis, A. I., Fayad, F., Kinsey, B. M., Sastry, K. S. and Adelstein, S. J. (1989) *Radiat. Res.*, **118**, 283–94.
12. Moser, H. E. and Dervan, P. B. (1987) *Science*, **238**, 645–50.
13. Voloshin, O. N., Mirkin, S. M., Lyamichev, V. I., Belotserkovskii, B. P. and Frank-Kamenetskii, M. D. (1988) *Nature*, **333**, 475–6.
14. Giovannangeli, C., Rougee, M., Garestier, T., Thuong, N. T. and Helene, C. (1992) *Proc. Natl Acad. Sci. U S A*, **89**, 8631–5.
15. Volkmann, S., Dannull, J. and Moelling, K. (1993) *Biochimie*, **75**, 71–8.
16. Panyutin, I. G. and Hsieh, P. (1993) *J. Mol. Biol.*, **230**, 413–424.
17. Maxam, A. M. and Gilbert, W. (1980) *Methods Enzymol.*, **65**, 499–525.
18. Mirkin, S. M. and Frank-Kamenetskii, M. D. (1994) *Annu. Rev. Biophys. Biomol. Struct.*, **23**, 541–576.
19. Lyamichev, V. I., Mirkin, S. M., Frank-Kamenetskii, M. D. and Cantor, C. R. (1988) *Nucleic Acids Res.* **16**, 2165–78.
20. Murray, V. and Martin, R. F. (1988) *J. Mol. Biol.*, **201**, 437–442.
21. Gibbs, R. A., Camakaris, J., Hodgson, G. S. and Martin, R. F. (1987) *Int. J. Radiat. Biol. Relat. Stud. Phys. Chem. Med.*, **51**, 193–9.
22. Kassis, A. I., Fayad, F., Kinsey, B. M., Sastry, K. S., Taube, R. A. and Adelstein, S. J. (1987) *Radiat. Res.*, **111**, 305–18.
23. Miyazaki, N. and Shinohara, K. (1993) *Radiat. Res.*, **133**, 182–6.